

Evolution of the Sensorimotor Control in an Autonomous Agent

Susanne A. Huber, Hanspeter A. Mallot, Heinrich H. Bülthoff

Max-Planck-Institut für biologische Kybernetik

Spemannstr. 38, 72076 Tübingen, Germany.

phone: ++49 (0)7071 - 601 - 608/603/600

fax: ++49 (0)7071 - 601 - 616

email: huber/ham/hhb@mpik-tueb.mpg.de

Abstract

Visually guided agents are introduced, that evolve their sensor orientations and sensorimotor coupling in a simulated evolution. The work builds on neurobiological results from various aspects of insect navigation and the architecture of the “Vehicles” of Braitenberg (1984). Flies have specialized visuomotor programs for tasks like compensating for deviations from the course, tracking, and landing, which involve the analysis of visual motion information. We use genetic algorithms to evolve the obstacle avoidance behavior. The sensor orientations and the transmission weights between sensor input and motor output evolve with the sensors and motors acting in a closed loop of perception and action. The influence of the crossover and mutation probabilities on the outcome of the simulations, specifically the maximum fitness and the convergence of the population are tested.

1 Introduction

In this work autonomous agents are introduced which navigate through a virtual world. Genetic algorithms are applied to evolve their visually guided control mechanisms and generate a sensorimotor coupling which enables them to survive in the environment. In particular, the behavioral module for obstacle avoidance is studied. For the task a visuomotor program is generated with the sensors and effectors acting in a closed loop of perception and action, thus effecting a permanent sensorimotor interaction.

In information processing the architecture of autonomous systems is decomposed into a chain of functional modules such as perception, information processing in a central unit and the execution and output of information. In other approaches the architecture is decomposed into task-achieving modules, which, in combination, produce the complex, “emergent” behavior of biological (Tinbergen, 1953) and artificial systems (Brooks, 1986; Flynn & Brooks, 1989). Starting from the assumption that perception and action – sensor input and motor control –

did not develop independently from each other, but are a coupled system – they have to be investigated in a closed loop. Braitenberg demonstrated with his “Vehicles” that even with simple architectures, it is possible to conceive of autonomous agents that can exhibit complex emergent behavior.

By studying the behavior of insects and the underlying neural mechanisms (for review see Egelhaaf & Borst, 1993), the architecture of biological navigation systems has been investigated. For our agent, the most important biological insight is that insects navigate mostly by evaluating visual motion information by means of neurons tuned to specific motion patterns (matched filters). The spatial localization of the receptive fields of these neurons is optimized with respect to certain behavioral tasks.

Franceschini and his colleagues demonstrate that the principle of motion vision can be used for navigational tasks in simulated and real agents (Franceschini, Pichon & Blanes, 1992). Cliff, Husbands and Harvey (1994) show the efficacy of using genetic algorithms to evolve concurrently the visual morphology along with the control networks. Here, we attempt to combine these approaches by evolving a competence for obstacle avoidance through simultaneous adaptation of sensor parameters and the sensorimotor coupling.

In the section 2, results from the research on the visual system of flies are reviewed and in section 3 the architectures of two types of autonomous agents are described. In section 4 the genetic algorithms used here are introduced, followed by the results of the simulations.

2 Perception of motion and visuomotor control in flies

The resolution of the compound eyes of flies is much coarser than that of human eyes and thus the perception of shape is more difficult. Hence, for visual orientation the detection of motion plays a more prominent role. While the insect is navigating through a stationary environment the images on the retinae are con-

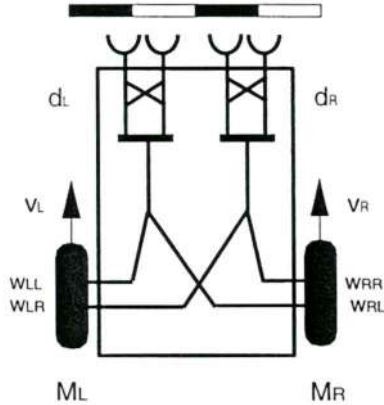


Figure 2: The agent has four sensors, the orientations of which is given by the angles azimuth Φ and inclination Θ . The outputs of these detectors d_L and d_R are connected to the motors M_L and M_R via the sensorimotor coupling.

between sensors and motors for different types of behaviors.

The input to each sensor is computed by “ray tracing” (Foley et al., 1987) where the intensities of single points – at the intersection of the line of sight with the visible surfaces – are averaged over a given number of sampling points. The orientations of the optical axes of the two sensors on one hemisphere of the visual field are evolved by the genetic algorithm. The other pair of sensors is positioned bilaterally symmetric on the other hemisphere. The time constants of the lowpass filters of the correlation motion detector are fixed ($\tau_{LP1} = 2.0s$, $\tau_{LP2} = 5.0s$). The matrix

$$\mathbf{W} = \begin{pmatrix} w_{LL} & w_{LR} \\ w_{RL} & w_{RR} \end{pmatrix} \quad (1)$$

contains the transmission weights for the sensorimotor coupling of the outputs d_L and d_R of the two motion-detectors with the two motors M_L and M_R . The velocity of the system is proportional to the force of the two motors, each motor producing a basic velocity v_0 which is modulated by the visual information:

$$\begin{pmatrix} v_L \\ v_R \end{pmatrix} = \mathbf{v}_0 - \mathbf{W} \begin{pmatrix} d_L \\ d_R \end{pmatrix}. \quad (2)$$

The velocity V in the heading direction and the angular velocity are:

$$V = \frac{1}{2}(v_L + v_R) \quad \text{and} \quad \dot{\varphi} = \frac{v_L - v_R}{c}. \quad (3)$$

where $c = 10\text{cm}$ is the distance between the wheels. The system has two degrees of freedom: rotation around the vertical axis and translation in the heading direction. In the simulations the numerical accuracy is set to 10^{-6} simulating a small amount of noise.

3.1 Agent of type 1:

Here the angular aperture of each sensor is 10° azimuth \times 10° elevation. We average the intensity of 10×10 sampling points to compute the visual input to each sensor. The basic velocity of the two motors is constant at $v_0 = 10\text{cm/s}$.

The agent moves through a tunnel which has a sinusoidal pattern ($\lambda = 1\text{m}$) mapped onto the walls, the floor and the ceiling. The width and height of the tunnel are 6m , the length is 100m . The elevation of the agent in the tunnel is kept constant at 3m . During evolution the system has to avoid two walls in the tunnel and maintain a safe distance of 15cm while navigating around the obstacles. The two walls are at $x = 15.0\text{m}$, $0.0\text{m} \leq y \leq 3.0\text{m}$ and $x = 35.0\text{m}$, $-3.0\text{m} \leq y \leq 0.0\text{m}$.

3.2 Agent of type 2:

For the agent of type 2 bilateral symmetry is assumed for the orientation of the motion detectors – as for agent of type 1 – and in addition for the transmission weights from the detector outputs to the motors. The angular aperture – being the same for all four sensors – is evolved. In order to keep the simulation time small, horizontal line sensors are used. The number of sampling points varies with the angular aperture of the sensors, the sampling base is kept constant at 1° . In addition the constant basic velocity v_0 of the two motors is a parameter optimized during evolution.

We run two blocks of simulations: in block 1 a sinusoidal pattern with the wavelength $\lambda = 2\text{m}$ is mapped onto the walls, ceiling and floor. Here the tunnel is 110m long and closed by a wall at both ends, the width and height is 4m . Four additional walls are placed at $x = 9\text{m}, 50\text{m}; 0.0\text{m} \leq y \leq 2.0\text{m}$ and $x = 19\text{m}, 80\text{m}; -2.0\text{m} \leq y \leq 0.0\text{m}$. The agent maintains a constant height of 2m .

In block 2 a random-dot pattern is used and walls are placed at $x = 9\text{m}, 50\text{m}; 0.0\text{m} \leq y \leq 2.0\text{m}$ and $x = 25\text{m}, 80\text{m}; -2.0\text{m} \leq y \leq 0.0\text{m}$. The tunnel is open at the end. The agents have to maintain a safe distance of 10cm from the walls.

4 Simulated evolution

4.1 The genetic algorithm

In a simulated evolution – using genetic algorithms – the autonomous agents adapt to the environment by generating an obstacle avoidance behavior. The orientation of two sensors and the transmission weights for the sensorimotor coupling are evolved. These parameters are encoded as a Gray-coded bitstring. Starting with a random initial population of bitstrings, each new generation is obtained by the following procedure:

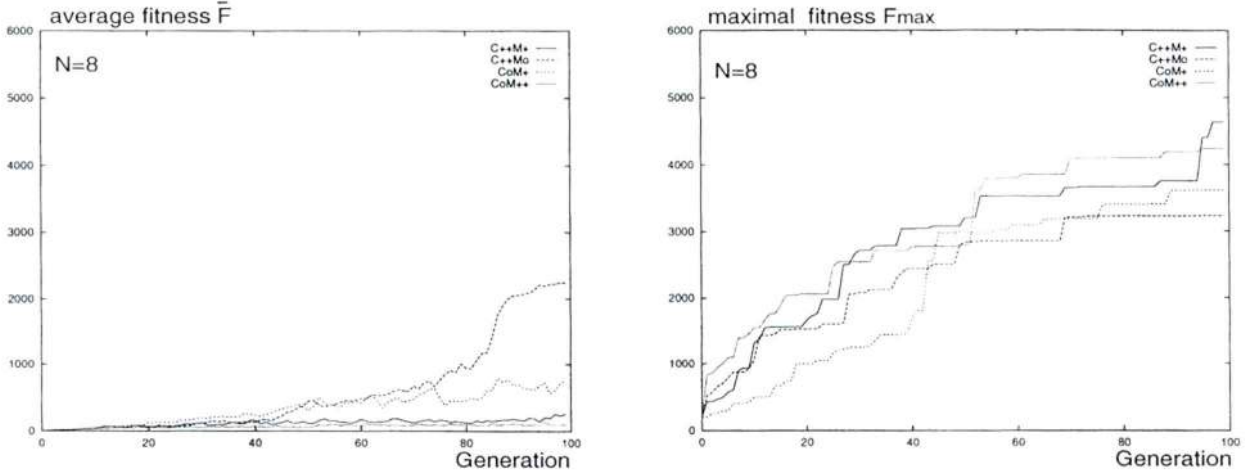


Figure 3: Average (left) and maximal (right) fitness, averaged over 8 trials.

4.4.1 Simulation block 1

The fitness function for the agent of type 2 in the simulation of block 1 is:

$$f = k s x_{max} \quad (8)$$

with $k = 1/2$ if the agent bumps into a wall and $k = 1$ if not. s is the length of the path the agent covers, and x_{max} the maximum value on the center axis of the tunnel the agent reached.

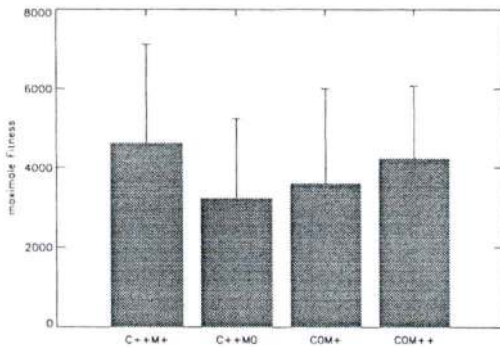


Figure 4: GA 1: Maximal fitness at generation 100, averaged over 8 trials.

4.4.2 Simulation block 2

Here the fitness function is:

$$f = k \sum_i |\Delta x_i| x_{max} \quad (9)$$

where $|\Delta x_i|$ is the distance on the center axis the agent covers in 10 steps. $|\Delta x_i|$ is computed every 10 steps and x_{max} is again the maximum value on the center axis of the tunnel the agent reached.

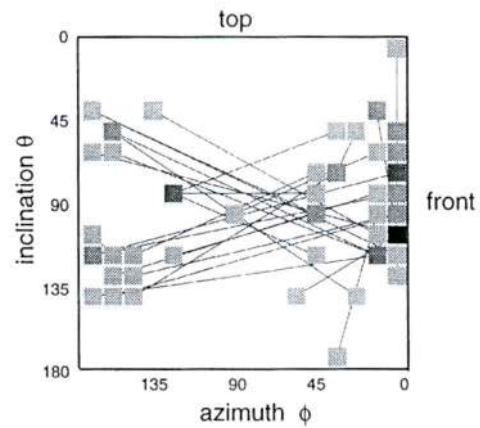


Figure 5: Distribution of the orientations of the sensors for the best individual of each trial. The sensors forming a detector are connected by a line. The intensity of the sensors code the frequency of their occurrence, with darker greyvalues being more frequently.

5 Simulations

5.1 Agent of type 1

In Fig. 3 the fitness F_{max} of the best individual and the average fitness \bar{F} of the population for every generation, both averaged over 8 trials are shown. As a high proportion of the individuals bump into the wall and get zero fitness, the average fitness is much smaller than the maximum fitness for all four conditions. The maximal fitness after 100 generations averaged over 8 trials (see Fig. 3) is not significantly different between the different mutation and crossover probabilities. The average fitness \bar{F} of the population is highest using only crossover followed by the $C_{++}M_{+}$ condition. The best individuals

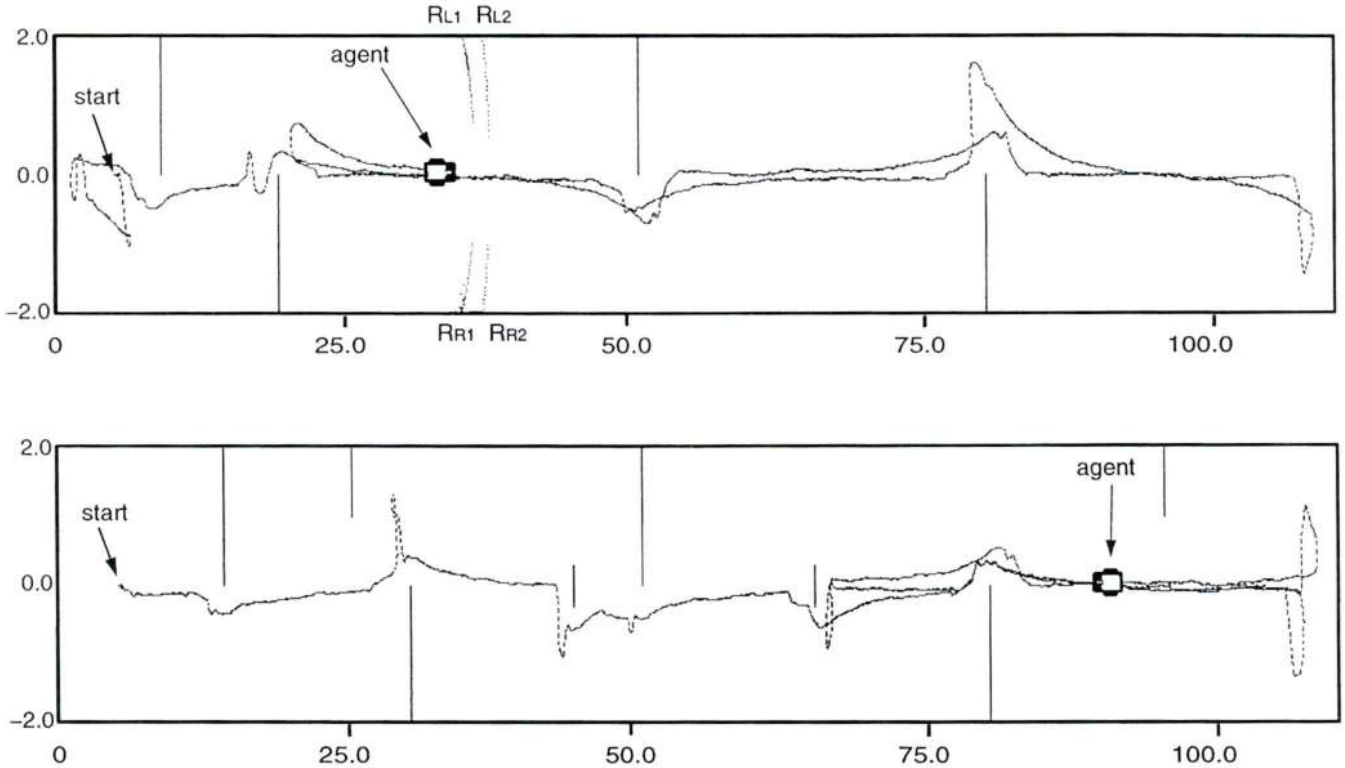


Figure 7: Path in tunnel 1 (top) and tunnel 2 (bottom). RR_1, RR_2 and RL_1, RL_2 in tunnel 1 indicate the lines of intersection of the sensor rays with the walls of the tunnel. Noise of $\pm 10\%$ is added to the input signals of the visual sensors and to the motor output. Sinusoidal pattern is mapped onto the walls ceiling and floor ($\lambda = 2$).

5.2 Agent of type 2

5.2.1 Simulation block 1

The agent of type 2 evolved in the simulation of block 1 (see Fig. 8) with the optical axes of its sensor orientations at 27.5° and 38.8° azimuth and 118.3° and 129.7° inclination. The evolved angular aperture of the sensors is with 27.5° much larger than for agent 1. The basic velocity of the motors is $v_0 = 6.2 \text{ cm/s}$. The resulting angular velocity is $\dot{\varphi} = -0.43(d_L + d_R)/c \text{ deg/s}$ and the velocity in the heading direction $V = v_0 + 0.16(d_L - d_R) \text{ cm/s}$. With this architecture the sensors of an agent moving on the center axis receive visual input mainly from the floor and from a small part of the side walls. If the agent approaches an obstacle, response is smaller for the motion detector nearer to the obstacle. As the preferred direction of the motion detectors is almost vertical and the sinusoidal pattern is oriented vertically the walls and horizontally on the floor, the change of intensity in the sensors and thus the perceived motion decreases as the agent approaches an obstacle. The transmission weights for the contralateral connections are stronger than for the ipsilateral connections, hence the reduction of the detector output has a stronger effect on the velocity of the motor on the contralateral side and the agent turns

away from the obstacle. The agents are tested in two different tunnels. Tunnel 1 is the original environment the agent evolved in, tunnel 2 differs in the number and position of the obstacles. Here we use 8 walls which are placed according to Fig. 7 (bottom). The test-trials are run with additional noise on sensor input and motor output. Table 2 describes the different noise conditions.

The agent has to survive 5000 time steps in the tunnel without bumping into a wall in order to show a successful behavior. With no additional noise the agent travels both tunnels in 100% of the time successfully. Adding more and more noise leads to a gradual reduction of performance. For tunnel 1 with $\pm 1\%$ noise, up to 70%–68% of the trials are successful, with $\pm 5\%$ 58–53% and with a high noise of 10% still 46%–38% do not bump into a wall during 5000 time steps. For the tunnel 2 the performance is reduced to 44%–31% for the different conditions. In Fig. 7 examples of a successful travel through the tunnel 1 and tunnel 2 with 10% noise on sensor input and motor output are shown.

5.2.2 Simulation block 2

Here the agent evolves two sensors with the same inclination and overlapping receptive fields (Fig. 10). The optical axes are at 28° and 17° azimuth and 106° inclina-

highest if only crossover is used. Comparing the average maximal fitnesses obtained after 100 generations the use of crossover and/or mutation leads to comparable optimization results.

In future work we will evolve agents navigating in more complex environments. We plan to increase the number of movement detectors and use an array of sensors forming a 360° field of view. The agent will evaluate the motion detected in this field of view with filters that respond maximal to certain motion patterns – e.g. rotation around the vertical axis and translation in the direction of heading. Those filters are derived from the tangential neurons (see sect. 2) found in the visual system of the fly's brain. In addition the agents will receive more degrees of freedom making 3D flight manoeuvres possible.

7 References

- [1] V. Braitenberg. *Vehicles – experiments in synthetic psychology*. The MIT Press, Cambridge, MA, 1984.
- [2] R. A. Brooks. A robust layered control system for a mobile robot. *IEEE Journal of Robotics and Automation*, RA-2: 14–23, 1986.
- [3] L. Davis (ed.). *Handbook of genetic algorithms*. Van Nostrand Reinhold, New York, 1991.
- [4] M. Egelhaaf, A. Borst. Motion computation and visual orientation in flies. *Comparative Biochemical Physiology*, 104 A/4: 659–673, 1993.
- [5] A. M. Flynn, R. A. Brooks. *Battling Reality*. MIT AI Memo 1148, 1989.
- [6] J. D. Foley, A. van Dam, S. K. Feiner, J. F. Hughes. *Computer Graphics – principles and practice*, Addison-Wesley, 1987.
- [7] S. Forrest. Genetic Algorithms: Principles of natural selection applied to computation. *Science*, 261: 872–878, 1993.
- [8] N. Franceschini, J. M. Pichon, C. Blanes. From insect vision to robot vision. *Philosophical Transactions of the Royal Society of London B* 337: 283–294, 1992.
- [9] K. G. Götz. Optomotorische Untersuchung des visuellen Systems einiger Augenmutanten der Fruchtfliege *Drosophila*. *Kybernetik*, 2: 77–92, 1964.
- [10] D. E. Goldberg. *Genetic algorithms in search, optimization, and machine learning*. Addison Wesley, Reading, Mass, 1989.
- [11] I. Harvey, P. Husbands, D. Cliff. Seeing the light: Artificial evolution, real vision. *Proceedings of the 3rd International Conference on Simulation of Adaptive Behavior*, 392–401, 1994.
- [12] B. Hassenstein, W. Reichardt. Systemtheoretische Analyse der Zeit-, Reihenfolgen- und Vorzeichenauswertung bei der Bewegungsperzeption des Rüsselkäfers *Chlorophanus*. *Zeitschrift für Naturforschung*, 11b: 513–524, 1956.
- [13] K. Hausen. Motion sensitive interneurons in the optomotor system of the fly. I. The horizontal cells: structure and signal. *Biological Cybernetics*. 45: 143–156, 1982.
- [14] R. Hengstenberg, H. Krapp, B. Hengstenberg. Visual sensation of self-motions in the blowfly *Calliphora*. In: *Biocybernetics of Vision: Integrative and Cognitive Processes* (ed.) C. Taddei-Ferretti (in press).
- [15] J. H. Holland. *Adaptation in natural and artificial systems*. The University of Michigan Press, Ann Arbor, 1975.
- [16] H. C. Longuet-Higgins, K. Prazdny. The interpretation of a moving retinal image. *Proceedings of the Royal Society of London B* 208: 385–397, 1980.
- [17] H. Mühlenbein. Evolution in time and space – the parallel genetic algorithm. *Foundations of Genetic Algorithms*, Morgan Kaufmann, San Mateo, CA, 1: 316–337, 1991.
- [18] W. Reichardt. Autocorrelation, a principle for the evaluation of sensory information by the central nervous system. In *Sensory Communication*: 303–317, ed: W. A. Rosenblith, The MIT Press and John Wiley and Sons, New York, 1961.
- [19] W. Reichardt. Functional characterization of neural interactions through an analysis of behavior. In *The neurosciences, fourth study program*: 81–104, ed: F. O. Schmitt, The MIT Press, London, 1979.
- [20] W. M. Spears. Crossover or Mutation? *Foundations of Genetic Algorithms*, Morgan Kaufmann, San Mateo, CA, 2:221–238, 1993.
- [21] N. Tinbergen. *Instinktlehre – vergleichende Erforschung angeborenen Verhaltens*. Parey Verlag, Berlin, Hamburg, 1953.
- [22] H. Wagner. Flight performance and visual control of flight of the free-flying housefly (*Musca domestica* L.), III. Interactions between angular movement induced by wide- and smallfield stimuli. *Philosophical Transactions of the Royal Society of London*, B 312: 581–595, 1986.
- [23] C. Wehrhahn, T. Poggio, H. Bülthoff. Tracking and chasing in houseflies (*Musca*). *Biological Cybernetics*, 45: 123–130, 1982.